Materials Chemistry and Physics 164 (2015) 71–77

Contents lists available at ScienceDirect

Materials Chemistry and Physics

journal homepage: www.elsevier.com/locate/matchemphys

Temperature influence on the synthesis of pristine graphene oxide and graphite oxide

Flavio Pendolino [a, *], Nerina Armata [b], Tiziana Masullo [c], Angela Cuttitta [c]

[a] Department of Industrial Engineering, University of Padova, Via Marzolo 9, 35131, Padova, Italy
[b] Department of Physics and Chemistry, University of Palermo, Viale delle Scienze, Ed. 17, 90128, Palermo, Italy
[c] Istituto per l'Ambiente Marino Costiero, Consiglio Nazionale delle Ricerche (IAMC-CNR), Via del Faro 3, 91021, Torretta Granitola Fz. Campobello di Mazara, TP, Italy

HIGHLIGHTS

- Temperature affects the expanded graphite exfoliation during the oxidation process.
- Graphene oxide is formed at moderate temperature.
- Graphite oxide is formed at low temperature.

GRAPHICAL ABSTRACT

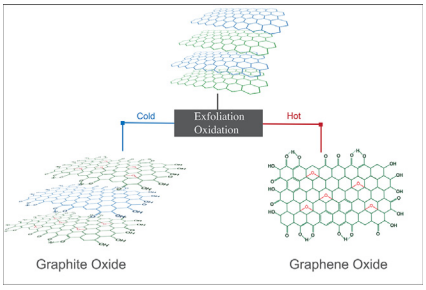

ARTICLE INFO

Article history:
Received 6 March 2015
Received in revised form
20 July 2015
Accepted 9 August 2015
Available online 28 August 2015

Keywords:
Nanostructures
Chemical synthesis
Monolayers
Multilayers

ABSTRACT

Derivative oxide carbon materials, such as graphene or graphite oxides, have been recently considered to be a promising material in a wide scenarios of emerging technologies due to their physical and chemical properties, as well as, for their low production costs. Even if apparently similar, these materials exhibit different physical and chemical properties. One of the critical issue is associated with the exfoliation process and contributes to the formation of graphene oxide and graphite oxide material. Here, we show a single synthetic wet method to produce graphene or graphite oxide by applying a control of the operational temperature during the reaction. The process was optimised to obtain the pristine graphite oxide at low temperature (T = 0 °C) and the pristine graphene oxide at higher temperature (T = 30 °C). Finally, the peculiar features of these materials were described using spectroscopic, structural and morphological measurements.

1. Introduction

Carbonaceous materials, such as nanotube, fullerenes, carbon fibres, are attracting attention due to their physical and chemical properties [1,2]. Recently, two oxide carbon derivatives, i.e. graphene oxide and graphite oxide, are understudy for their similar properties. The interest in graphene oxide (GO) grew in the context of finding a more suitable and scalable method for producing pristine graphene. Nevertheless, GO exhibits, in comparison with pristine graphene, distinct features which can be employed for novel applications. Graphene oxide consists of a two-dimensional plane bonded with oxygen domains which provide an amphiphilic character with carbon atom hybridization from sp^2 and sp^3

* Corresponding author.
E-mail address: flavio.pendolino@unipd.it (F. Pendolino).

http://dx.doi.org/10.1016/j.matchemphys.2015.08.024
0254-0584/

due to the binding of oxygen atoms into the graphene basal plane. The GO is a non-stoichiometric "molecule" because of its starting material (often expanded graphite) which influences the size of the basal plane of the final product [3–7]. Differently, graphite oxide (GtO) can be described as a "grain" of graphite where the surface is oxidized. In practice, the synthetic protocol consists of two main steps: exfoliation and oxidation. In the first step, each carbon layer is "peeling" from graphite grain by means of an exfoliation agent (often sulphuric acid). Then, the basal plane is oxidized by an oxidizing agent (commonly $KMnO_4$). A key issue on the wet synthesis of GO is the exfoliation step [8]. When the exfoliation step is not fully completed, a resulting GtO material is produced. This latter material has relevant properties such as an appreciable electric conductivity, which can be categorised in between graphene and graphene oxide. However, a lack of information on the behaviour of these materials causes a missing of a clear/standard synthetic procedure and mixing up the results of the characteristics of GO or GtO. Often, old literature reported the formation of graphene oxide as graphite oxide because of the little knowledge about the graphene and graphene derivatives materials around 2010. For example, under certain conditions of low number of non-exfoliated layers, GtO and GO exhibit similar spectroscopic features [9].

Essentially, three basic approaches, derived from Brodie method [5], are used as starting procedure for synthesizing GO (eventually GtO): Hummers [4], Staudenmaier [10] and Hofmann [3] methods. All of these methods produce graphene oxide by exfoliating and oxidizing of the graphite powder via chemical wet reactions. However, those procedures imply some limitations in the practical use [9,11,12]. First, the reactions involve hazardous reagents (e.g., sodium nitrate or potassium chlorate). Second, some reagents, such as sodium nitrate or fuming nitric acid, introduce heteroatoms or hole defects which affect the reactivity and the structural characteristic of GO [13,14]. Third, these methods are time-consuming (several days) with a low final yield. For these reasons, variation of Hummers-Staudenmaier-Hofmann methods have been investigated [6,15]. In the prospective of mass production of GO, Sun et al. [7] proposed a four steps protocol using a lower amount of exfoliating agent (sulphuric acid) with the positive consequence of getting high yield and quality GO. To the best of our knowledges, any clear distinction between the synthesis for graphene oxide and graphite oxide is reported and often GO dispersions consists of a mixture with GtO. Somehow, GtO is treated as undesirable product which affects the final GO yield.

The present paper is focused on the description of an alternative production method for graphene or graphite oxides, based on the four steps described in the Sun approach [7]. This approach has the advantage of producing high GO/GtO yield and allows a scale up production. Here, a single protocol is reported to synthesized both GO or GtO by only changing the operational temperature during the reaction. Our results provide experimental evidences concerning the difference of physical chemical properties of the final product of synthesis (GO and GtO) by taking advantage of handy techniques.

2. Experimental

2.1. Chemicals

The following chemicals were used as received: $KMnO_4$ (Sigma–Aldrich), H_2SO_4 (98%, Sigma–Aldrich), HCl (37%, Sigma–Aldrich), ECOPHIT 50 (size 40–50 μm, SGL GROUP).

2.2. Graphene oxide synthesis

The production of graphene oxide was carried out using a modification of the Sun protocol, described in our previous work [16]. Briefly, expanded graphite (2.5 g) and $KMnO_4$ (7 g) were introduced into a 500 mL beaker and stirred until homogeneity. The beaker was placed in an ice-bath and 50 mL of concentrated sulphuric acid (98%) were added slowly[1] with continuous stirring with magnetic stir bars until a paste (green-petrol colour) was obtained. The beaker was placed into a water bath at about 30 °C for 30 min to produce a spontaneous volumetric expansion. Next, the hydrolysis of the material was obtained adding 200 mL of distilled water very slowly in order to prevent an uncontrolled temperature increase. Then, the green-brownish liquid was placed in a water bath at 80 °C for 1 h to obtain a darker suspension. The warm suspension was paper filtered (2 μm pore size) and washed with 500 mL distilled water, 500 mL HCl 0.15 M (to remove Mn^{2+}) and finally with 500 mL distilled water. The presence of sulfate ions in the GO dispersions was checked by a $BaSO_4$ spot test. The solid samples were prepared by drying in an oven at 80 °C overnight.

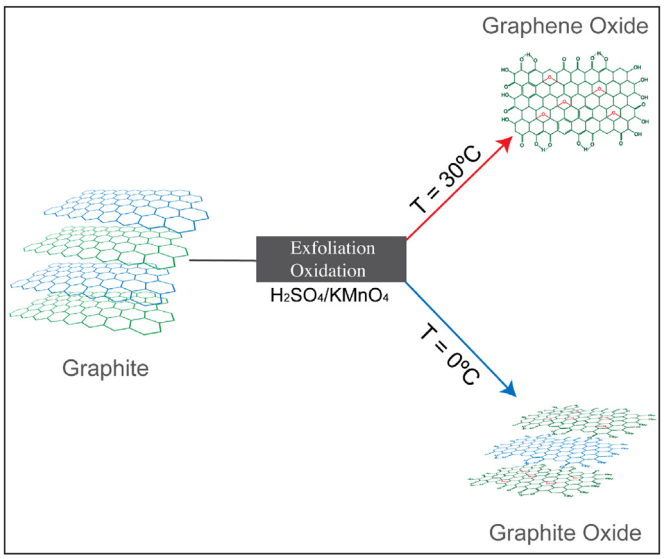

Fig. 1. Reaction scheme for the synthesis of graphene oxide and graphite oxide.

2.3. Graphite oxide synthesis

The synthesis of graphite oxide dispersion was carried out by means of lowering the operational temperature for the synthesis of graphene oxide. In practise, all the reagents were pre-cooled for about 2 h in an ice-bath. Then, the method follows each synthetic step described above except for maintaining the temperature as low as an ice-bath temperature during the entire synthesis process. For this reason some differences were encountered. First, the colour of the mixture were dark/black in all steps. Next, the volumetric expansion was suppressed [8], and, finally, the product appears as a powder-like instead of flaky material. The solid samples were prepared by drying in an oven at 80 °C overnight.

A scheme for the synthesis of graphene oxide and graphite oxide is shown in Fig. 1.

The direct observation of the two raw materials showed some peculiar difference: GO sample is a flake-like material that cannot be easily powdered when is treated with pestle and mortar and pasty material is obtained (may be due to the adsorption of

[1] The temperature is kept below 55 °C to prevent accidental explosion due to the presence of Mn_2O_7 in a solution of sulphuric acid.

humidity). On the opposite, GtO is very similar to expanded graphite with a grey-black powder.

2.4. Characterization

Diffraction measurements were performed with Bruker D8 Advance, Cu K_α radiation $\lambda = 0.15418$ nm. The interlayer distance was evaluated by the Bragg equation. UV–vis spectra were recorded in Jasco V/570 spectrometer with quartz cell. The solution is 0.1 mg/mL for both GO and GtO. FTIR measurements were performed out in Jasco FT/IR-620 spectrometer using KBr pellets with ratio sample/KBr of 1:100. The electrical resistance was measured by means of Keithley Multimeter 2400 4-wire on a pellet. The pellet, with size of 13 mm (diameter) and 1 mm hight, was made by pressing powder at 10 tons for 30 s (Fig. 4). The electric resistance was measured on the surface along a circle at a distance of 6 mm using clips to keep electrodes at the same distance and pressure. The value is the average of 10 measurements. Morphological images and microanalysis were recorded using a SEM (Philips XL30 TMP) integrated with EDX (PV9900). Photoluminescence measurements were performed on a RF 5301PC spectrofluorometer (Shimadzu) using 5/5 nm spectral slit bandwidth for excitation and emission. Wavelength scanning super (about 3000 nm/min) with high sensitivity selection. The S/N ratio of instrument is 150 or higher for the Raman line of distilled water (350 nm excitation wavelength, 5 nm spectral bandwidth, and 2 s response for 98% of the full scale). Wavelength accuracy is ±1.5 nm. Emission spectra were recorded at the maximum and optimal excitation wavelengths. Samples were prepared by dispersing the solid in milliQ water (1 mg/mL, pH 7) and sonicating for 15 min at RT. The dispersions were stirred for 1 h at 300 rpm and centrifugate for 5 min at 10,000 rpm before analysing the soluble fractions.

3. Results and discussion

Diffractograms of (*a*) graphene oxide and (*b*) graphite oxide are shown in Fig. 2. The GO shows a peak centred at 11.2°, which is associated with the variation of the interlayer distance (d = 0.8 nm) due to the presence of chemical groups onto the graphene basal plane. This is consistent with the range values of 9°–12° reported in the literature [13,17–20].

Besides, the spectrum of GtO (Fig. 2b) has a broader peak centred at 26.2° with an interlayer distance of d = 0.35 nm, comparable with the interlayer distance of the expanded graphite. The expanded graphite diffractogram (Fig. 2c) is reported as a reference and exhibits its characteristic narrow diffraction peak at $2\theta = 26.5°$. The correlation of XRD with single and multilayer was demonstrated by Dakin et al. [21] and Xu et al. [22] and this is in accordance with our experiments.

Morphological aspects of GO and GtO are investigated by using scanning electron microscope (SEM), as shown in Fig. 3. Here, the pristine expanded graphite (Fig. 3a and d) is displayed and exhibits large grains with an average size of about 50 μm. Similarly, GtO appears as grain-like shape and homogeneously distributed (Fig. 3b and e). Unlikely, GO morphology consists of tightly packed layers, as shown in Fig. 3c and f. The distinct morphology is related to the exfoliation process in the first step of synthesis and the re-packing of the material in the solid phase due to the oxygen domains on the graphene basal plane. The elemental analysis is evaluated from energy dispersive X-ray (EDX). Comparable amount of oxygen is archived for GO (~22%) and GtO (~24%).

The ratio carbon/oxygen (C/O) is strongly depended on the GO synthesis as reported in literature [1,6,11,23]. In our experiments the C/O ratio is resulted in 3.6 and 3 for GO and GtO, respectively. In Table 1 is shown the comparison of our results and Hammers, Brodie, Sun and Staudenmaier methods from several authors (some of the most cited). As observed, the majority of references archived a C/O ratio around 2.2, implying a high oxidized graphene. Instead, from our data, a less oxidized sample is found and this affects the GO properties, e.g. a higher interlayer distance at the angle of 11.2° in comparison with the average value that is around 9–10°, or a FTIR spectrum.

The resistivity (ρ) is measured for expanded graphite, GtO and GO on a pellet (Fig. 4). The expanded graphite shows a resistivity of $0.28 \pm 0.01\ \Omega$ m (3.5 ± 0.1 S/m) [32]. By contrast GO exhibits a high resistivity of about $2.3 \pm 0.1 \times 10^7\ \Omega$ m ($4.3 \pm 0.1 \times 10^{-7}$ S/m) [1,6,11]. Finally, the resistivity of GtO is $1.78 \pm 0.01\ \Omega$ m (0.56 ± 0.01 S/m). A comparison of resistivity for several main synthetic methods is reported in Table 1.

Fig. 5 shows FTIR spectra for the GO and GtO dispersions. The spectrum for GO (Fig. 5a) was described in details in our previous work [33]. Briefly, the characteristic broad band at 3439 cm^{-1} corresponds to the stretching vibrations of bonded O–H. The tiny doublet peaks at 2920 cm^{-1} and 2850 cm^{-1} correspond to the symmetric and antisymmetric stretching vibrations of $-CH_2$. The peak at 1710 cm^{-1}, corresponding to the C=O stretching vibration [13,17–20,34], while the peak at 1620 cm^{-1} is sometimes assigned to the O–H vibrations due to the presence of adsorbed water [19]. We have interpreted [16,33] those peaks as *keto-enol tautomerism*. The peak at 1384 cm^{-1} could correspond to the bending vibration of O–H for the alcohols. The peak at 1090 cm^{-1} may be interpreted as referring to the epoxy group, however, it is more likely related to the stretching vibration of C–O for alcoholic group or alkoxy (R–O). In Fig. 5b is shown the spectrum for GtO where no appreciable discrepancies are observed. However, both spectra differ in a few features. First, the presence of an additional peak at 1716 cm^{-1} is observed and corresponding to C=O stretching vibration for an

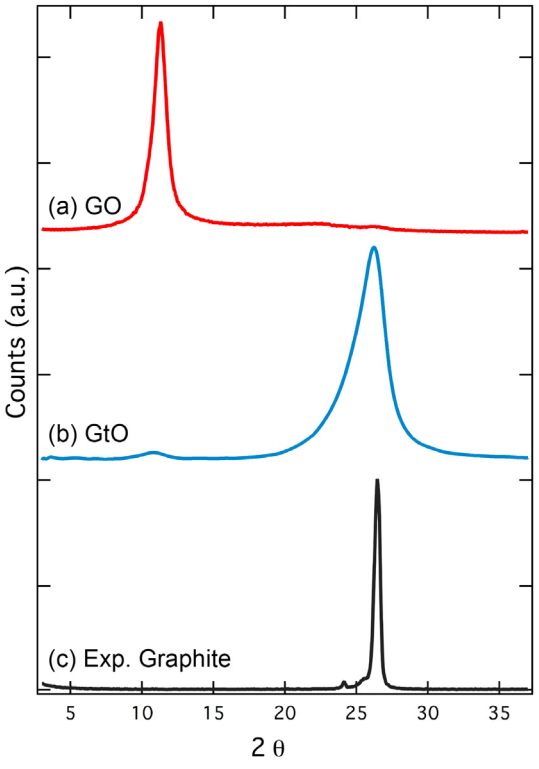

Fig. 2. X-ray diffraction data for the (*a*) GO, (*b*) GtO and (*c*) expanded graphite.

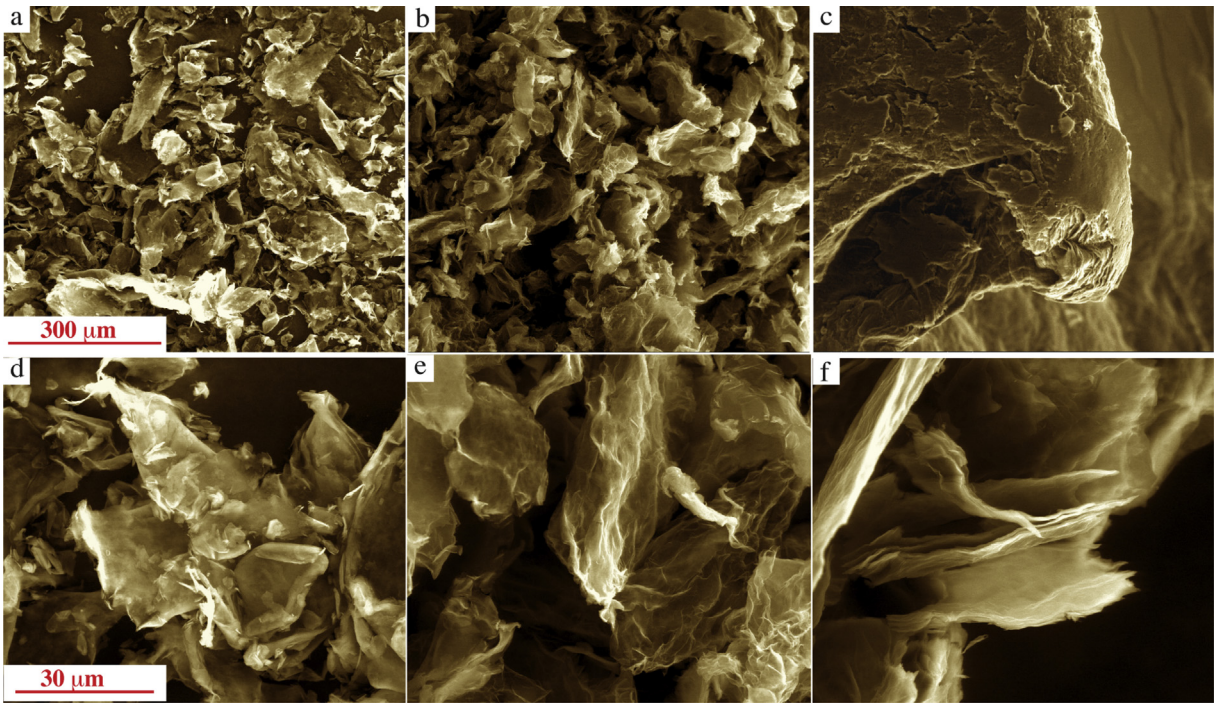

Fig. 3. SEM images of (*a*) expanded graphite, (*b*) GtO and (*c*) GO. Higher resolved SEM images are reported in *d*, *e* and *f*, respectively for *a*, *b* and *c*. Red marks indicate 300 μm for (a–c) and 7 μm for (d–f) images. (For interpretation of the references to colour in this figure legend, the reader is referred to the web version of this article.)

Table 1
Carbon-oxygen ratio (C/O) for graphene oxide using Brodie, Staudenmaier, Hummers, Modified Hummers and Sun methods. The amount of oxygen decreases along the table. Resistivity is reported for several synthetic methods.

Method	C/O	Resistivity 10^5 Ω m	Ref
Mod. Hummers	0.7–1.3	0.2–1000	[6,24,25]
Hummers	1.8–2.5	0.005–0.01	[4,23,26–28]
Staudenmaier	2.2	120	[10,26,29]
Sun	2.5	0.18	[7]
Brodie	2.4–2.9	0.15–60	[5,23,26,30,31]
This work (GO)	3.5	230	

aliphatic ketone. Next, the intensity of the peak at 1384 cm^{-1} is greater comparing with the GO spectrum and may be related to the peak at 1716 cm^{-1}. Finally, the peaks at 1635 cm^{-1} and 1584 cm^{-1} are interpreted as the keto-enol equilibrium.

UV–vis spectra for GO and GtO in the range 190–900 nm are investigated in water solution and reported in Fig. 6. As we can observe, the region 400–900 nm is not affected by absorptions. The maximum absorbance for GO (Fig. 6a) takes place at $\lambda_{Max} = 230$ nm. This band is attributed to $\pi \rightarrow \pi^{\star}$ transitions in conjugated systems [34,35]. A shoulder is present at around $\lambda = 290$ nm and is often assigned to the $n \rightarrow \pi^{\star}$ transition of a carbonyl group. A change of the optical absorption is found in the GtO spectrum (Fig. 6b) due to the oxygen domains present on the graphite. Here, the shoulder at 290 nm disappears probably due to a less number of conjugated systems with carbonyls. Besides, the maximum absorbance is shifted to lower wavelengths (196 nm). This fact is reported by Lai et al. [36], who investigated the variation of the UV–vis spectra with the number of layers of graphene oxide. The authors claimed, using UV–vis and AFM techniques, that for the monolayer is

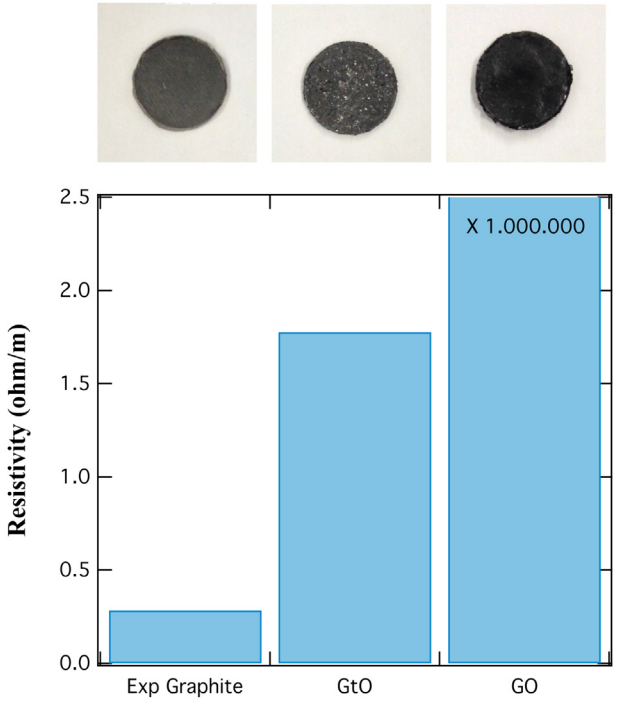

Fig. 4. Digital photographs of pellets and resistivity chart for expanded graphite, graphite oxide (GtO) and graphene oxide (GO).

observed a corresponding UV–vis spectrum with a maximum absorbance at 230 nm and a shoulder around 300 nm. When the number of non-exfoliated layers are increased, the shoulder

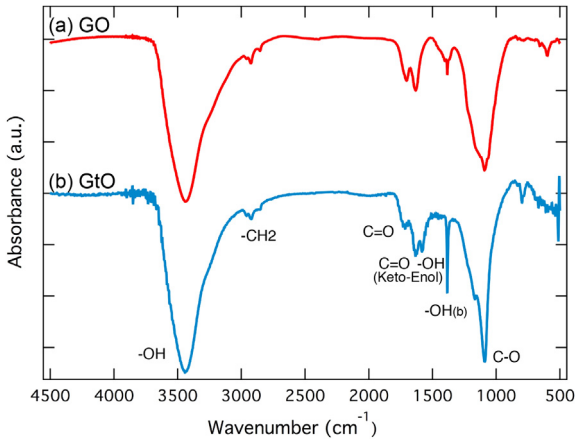

Fig. 5. FTIR spectra for (*a*) GO and (*b*) GtO after drying fresh water dispersions.

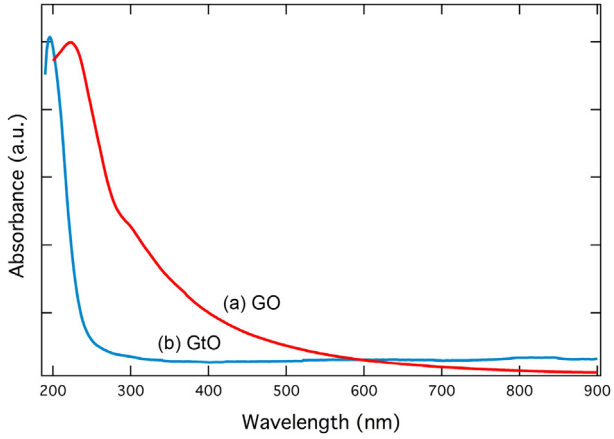

Fig. 6. UV–vis spectra of the (*a*) GO and (*b*) GtO in water solution.

disappears and maximum peak vanishes for thick-layer >10 layers. Comparing Lai's conclusions and our UV–vis results, we can argue to have graphene oxide and graphite oxide. This result is also supporting diffraction data (Fig. 2) where the GtO interlayer distance is comparable with the expanded graphite confirming that the exfoliation is negligible.

The photoluminescence (PL) of GO and GtO is shown in Fig. 7 and is ranged from 350 nm to 590 nm showing, in the majority of cases, a broad band of the spectrum. The origin of this phenomenon for oxidizing carbon materials is still unknown but it can be attributed to the conjugated systems. Several parameters affect the photoluminescence signals such as pH [37,38] or reduction [37–41] and the C/O ratio, due to the oxygen domains in the structure, seems affect the PL signals [37–42]. Nevertheless, the photoluminescence can discriminate between GO and GtO spectrum. The contour plot of GO is reported in Fig. 7a using an excitation wavelength (λ_{ex}) in the range 280–400 nm. The red colour identifies the maximum GO emission (447 nm) at $\lambda_{ex} = 330$ nm. At same excitation wavelength, GtO has maximum emission at 447 nm (Fig. 7b). Above $\lambda_{ex} = 400$ nm, no emission signal is recorded. In Fig. 7c and d selected spectra are extracted from the contour plot at 280 nm, 300 nm, 330 nm and 350 nm. Here, it is possible to distinguish the shape of photoluminescence bands which appear broad for 280 nm, 300 nm and 350 nm but a more narrow shape with a high emission intensity is found at 330 nm. Fig. 7c, the position of maximum emission peak λ_{em} are kept constant when the excitation wavelength is changed. By comparing GO and GtO spectra at $\lambda_{ex} = 300$ nm (Fig. 7f), it is interesting to note that the position of the maximum is shifted from 447 nm to 453 nm (6 nm). This event is not observed for all excitation wavelengths (Fig. 7e) where the maximum peak position is unchanged. The intensity of the photoluminescence is higher for GtO comparing with GO and is probably attributed to the heterogenous electronic structures with a variable sp^2 and sp^3 hybridization, as reported by Chien et al. [41].

4. Conclusions

To conclude, this work leads to the synthesis of graphene oxide and graphite oxides by means of a single wet procedure. The method described in this paper consists of changing the operational temperature. Low temperature (T = 0 °C) affects the exfoliation process producing a graphite oxide, while high temperature (T = 30 °C) helping the process and a single layer graphene oxide is formed. GO and GtO show distinct physical chemical features which can be identified by routinely laboratory techniques, such as spectroscopic and morphological/structural analysis. From direct observation, the raw material gives information about the nature of the product, i.e. powder and dark/black for GtO and brownish and flake-like for GO. The crystallographic data reveal the degree of exfoliation of the material estimating the interlayer distance. Larger plane distance (~0.8 nm) is found when GO layer is overlapped to each other to form a stack-pile structure (in the dry sample) due to the interaction between oxygen domains and π-system. On contrary, a smaller interlayer distance can be observed for a GtO where the plane distance is still similar to the pristine graphite value (0.35 nm). The morphology is observed using SEM analysis bearing a different microscopic structure, where a layered arrangement of the GO and particles distribution of GtO were recognised. A straightforward indicator to discriminate GO from GtO consists in the analysis of the shape and maximum absorbance of UV–vis spectra. The presence of a peak at 230 nm with a shoulder around 300 nm with a broader peak is an indication of GO, in contrast with GtO where a sharp spectrum is observed without any shoulder signals ($\lambda = 195$ nm, sharp peak). Furthermore, photoluminescence analysis dealt with a characteristic spectrum brings to a greater intensity for GtO over GO and archiving a difference in the PL signal (6 nm) of the maximum of emission at $\lambda_{ex} = 300$ nm. Few differences are noticed in FTIR data. The reason for that resides on the fact that the functional groups on the surface of GO or the GtO are similar, hence, their spectra are almost identical. However, an additional carbonyl (1716 cm^{-1}) is found and more intense and sharp signal for the frequencies of C–O groups is looked in the GtO spectrum. Finally, electric conductivity simply distinguishes GO (good insulator) from GtO (conductive material). The present study is a step forward to set out a standard protocol for the production of oxidized carbon materials and help researchers in distinguishing pristine GO and GtO materials from incomplete synthesis or mixtures.

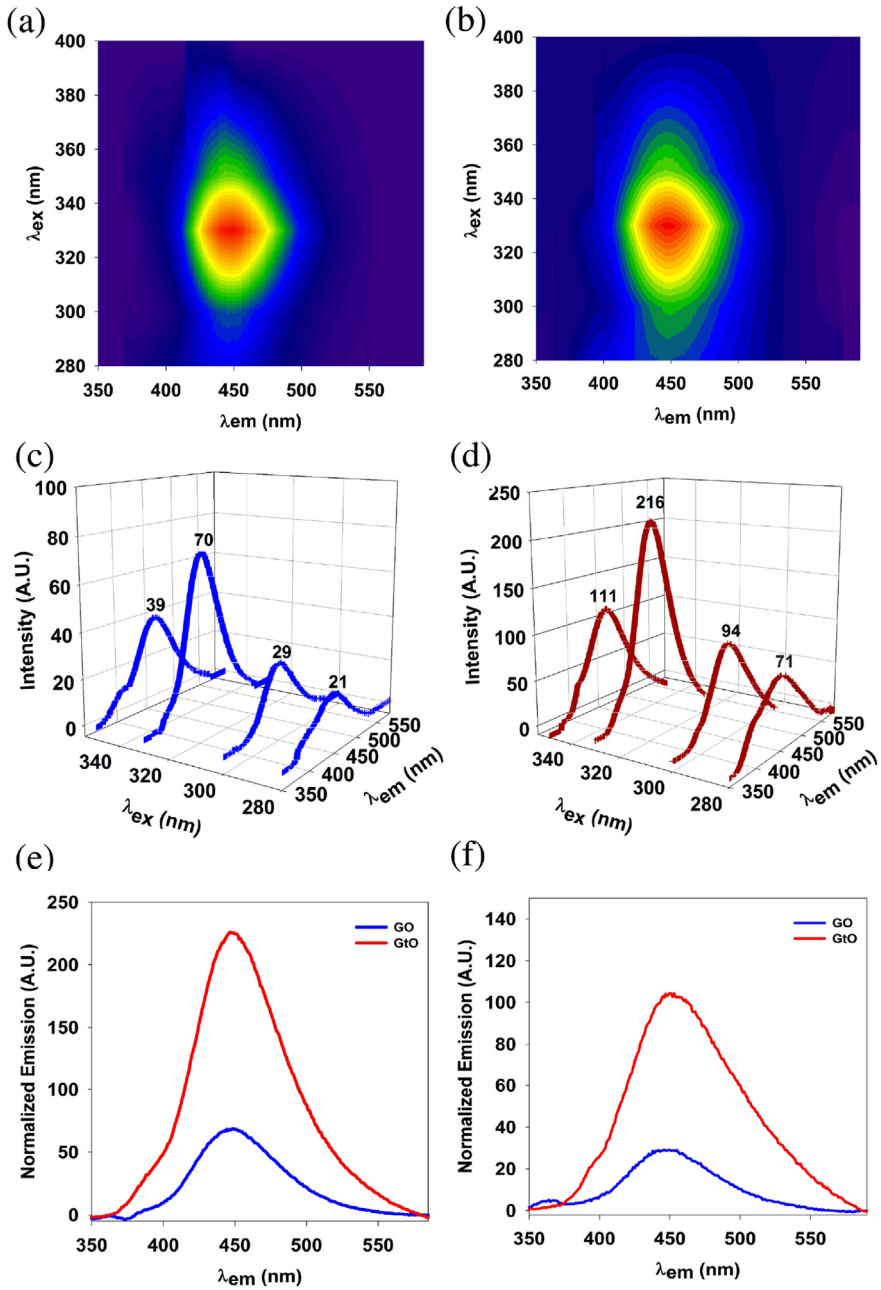

Fig. 7. Photoluminescence (PL) spectra for GtO (right) and GO (left) in the range $\lambda_{ex} = 280–350$ nm and $\lambda_{em} = 350–590$ nm. (a–b) PL excitation-emission map of GO and GtO. (c–d) GO and GtO plots at $\lambda_{ex} = 280$ nm, 300 nm, 330 nm, 350 nm. (e) PL spectra comparison of GO and GtO fixing at $\lambda_{ex} = 330$ nm, (f) PL spectra comparison of GO and GtO fixing at $\lambda_{ex} = 300$ nm.

Acknowledgement

This work was supported by 'Progetto Strategico MAESTRA' funded by the University of Padova.

References

[1] O.C. Compton, S.T. Nguyen, Graphene oxide, highly reduced graphene oxide, and graphene: versatile building blocks for carbon-based materials, Small 6 (2010) 711–723.
[2] C. Su, K.P. Loh, Carbocatalysts: graphene oxide and its derivatives, Acc. Chem. Res. 46 (2013) 2275–2285.
[3] U. Hofmann, E. König, Untersuchungen über Graphitoxyd, Z. Anorg. Allg. Chem. 234 (1937) 311–336.
[4] W.S. Hummers, R.E. Offeman, Preparation of graphitic oxide, J. Am. Chem. Soc. 80 (1958), 1339–1339.
[5] B.C. Brodie, On the atomic weight of graphite, Philos. Trans. R. Soc. Lond. 149 (1859) 249–259.
[6] D.C. Marcano, D.V. Kosynkin, J.M. Berlin, A. Sinitskii, Z. Sun, A. Slesarev, L.B. Alemany, W. Lu, J.M. Tour, Improved synthesis of graphene oxide, ACS Nano 4 (2010) 4806–4814.
[7] L. Sun, B. Fugetsu, Mass production of graphene oxide from expanded graphite, Mater. Lett. 109 (2013) 207–210.
[8] D.W. Boukhvalov, Oxidation of a graphite surface: the role of water, J. Phys. Chem. C 118 (2014) 27594–27598.
[9] D.R. Dreyer, S. Park, C.W. Bielawski, R.S. Ruoff, The chemistry of graphene oxide, Chem. Soc. Rev. 39 (2010) 228–240.
[10] L. Staudenmaier, Verfahren zur Darstellung der Graphitsäure, Ber. Dtsch. Chem. Ges. 31 (1898) 1481–1487.
[11] D.R. Dreyer, A.D. Todd, C.W. Bielawski, Harnessing the chemistry of graphene oxide, Chem. Soc. Rev. 43 (2014) 5288–5301.
[12] J. Guerrero-Contreras, F. Caballero-Briones, Graphene oxide powders with

different oxidation degree, prepared by synthesis variations of the Hummers method, Mater. Chem. Phys. 153 (2015) 209–220.
[13] A.M. Dimiev, J.M. Tour, Mechanism of graphene oxide formation, ACS Nano 8 (2014) 3060–3068.
[14] C.K. Chua, M. Pumera, Chemical reduction of graphene oxide: a synthetic chemistry viewpoint, Chem. Soc. Rev. 43 (2014) 291–312.
[15] H. Yang, Y. Hernandez, A. Schlierf, A. Felten, A. Eckmann, S. Johal, P. Louette, J.J. Pireaux, X. Feng, K. Müllen, V. Palermo, C. Casiraghi, A simple method for graphene production based on exfoliation of graphite in water using 1-pyrenesulfonic acid sodium salt, Carbon 53 (2013) 357–365.
[16] F. Pendolino, G. Capurso, A. Maddalena, S. Lo Russo, The structural change of graphene oxide in a methanol dispersion, RSC Adv. 4 (2014) 32914–32917.
[17] D.W. Lee, L. De Los Santos, V.,J.W. Seo, L.L. Felix, A. Bustamante, D.,J.M. Cole, C.H.W. Barnes, The structure of graphite oxide: investigation of its surface chemical groups, J. Phys. Chem. B 114 (2010) 5723–5728.
[18] T.-F. Yeh, J.-M. Syu, C. Cheng, T.-H. Chang, H. Teng, Graphite oxide as a photocatalyst for hydrogen production from water, Adv. Funct. Mater. 20 (2010) 2255–2262.
[19] A. Kaniyoor, T.T. Baby, S. Ramaprabhu, Graphene synthesis via hydrogen induced low temperature exfoliation of graphite oxide, J. Mater. Chem. 20 (2010) 8467–8469.
[20] B. Shen, D. Lu, W. Zhai, W. Zheng, Synthesis of graphene by low-temperature exfoliation and reduction of graphite oxide under ambient atmosphere, J. Mater. Chem. C 1 (2013) 50–53.
[21] D. a Dikin, S. Stankovich, E.J. Zimney, R.D. Piner, G.H.B. Dommett, G. Evmenenko, S.T. Nguyen, R.S. Ruoff, Preparation and characterization of graphene oxide paper, Nature 448 (2007) 457–460.
[22] P. Xu, Y. Yang, S.D. Barber, J.K. Schoelz, D. Qi, M.L. Ackerman, L. Bellaiche, P.M. Thibado, New scanning tunneling microscopy technique enables systematic study of the unique electronic transition from graphite to graphene, Carbon 50 (2012) 4633–4639.
[23] S. You, S.M. Luzan, T. Szabó, A.V. Talyzin, Effect of synthesis method on solvation and exfoliation of graphite oxide, Carbon 52 (2013) 171–180.
[24] N.I. Kovtyukhova, P.J. Ollivier, B.R. Martin, T.E. Mallouk, S.A. Chizhik, E.V. Buzaneva, A.D. Gorchinskiy, Layer-by-layer assembly of ultrathin composite films from micron-sized graphite oxide sheets and polycations, Chem. Mater. 11 (1999) 771–778.
[25] S. Gilje, S. Han, M. Wang, K.L. Wang, R.B. Kaner, A chemical route to graphene for device applications, Nano Lett. 7 (2007) 3394–3398.
[26] W. Scholz, H.P. Boehm, Untersuchungen am Graphitoxid. VI. Betrachtungen zur Struktur des Graphitoxids, Z. Anorg. Allg. Chem. 369 (1969) 327–340.
[27] S. Stankovich, D. a Dikin, R.D. Piner, K.A. Kohlhaas, A. Kleinhammes, Y. Jia, Y. Wu, S.T. Nguyen, R.S. Ruoff, Synthesis of graphene-based nanosheets via chemical reduction of exfoliated graphite oxide, Carbon 45 (2007) 1558–1565.
[28] I. Jung, D.A. Field, N.J. Clark, Y. Zhu, D. Yang, R.D. Piner, S. Stankovich, D. a Dikin, H. Geisler, J. Carl A Ventrice, R.S. Ruoff, Reduction kinetics of graphene oxide determined by electrical transport measurements and temperature programmed desorption, J. Phys. Chem. C 113 (2009) 18480–18486.
[29] H.-L. Ma, H.-B. Zhang, Q.-H. Hu, W.-J. Li, Z.-G. Jiang, Z.-Z. Yu, A. Dasari, Functionalization and reduction of graphene oxide with p-phenylene diamine for electrically conductive and thermally stable polystyrene composites, ACS Appl. Mater. Interfaces 4 (2012) 1948–1953.
[30] H.-J. Shin, K.K. Kim, A. Benayad, S.-M. Yoon, H.K. Park, I.-S. Jung, M.H. Jin, H.-K. Jeong, J.M. Kim, J.-Y. Choi, Y.H. Lee, Efficient reduction of graphite oxide by sodium borohydride and its effect on electrical conductance, Adv. Funct. Mater. 19 (2009) 1987–1992.
[31] H.C. Schniepp, J.-L. Li, M.J. McAllister, H. Sai, M. Herrera-Alonso, D.H. Adamson, R.K. Prud'homme, R. Car, D.A. Saville, I.A. Aksay, Functionalized single graphene sheets derived from splitting graphite oxide, J. Phys. Chem. 110 (2006) 8535–8539.
[32] D.D.L. Chung, Exfoliation of graphite, J. Mater. Sci. 22 (1987), 4190–4198–4198.
[33] F. Pendolino, E. Parisini, S. Lo Russo, Time-dependent structure and solubilization kinetics of graphene oxide in methanol and water dispersions, J. Phys. Chem. C 118 (2014) 28162–28169.
[34] H. Cao, X. Wu, G. Yin, J.H. Warner, Synthesis of adenine-modified reduced graphene oxide nanosheets, Inorg. Chem. 51 (2012) 2954–2960.
[35] J.I. Paredes, S. Villar-Rodil, A. Martínez-Alonso, J.M.D. Tascón, Graphene oxide dispersions in organic solvents, Langmuir 24 (2008) 10560–10564.
[36] Q. Lai, S. Zhu, X. Luo, M. Zou, S. Huang, Ultraviolet-visible spectroscopy of graphene oxides, AIP Adv. 2 (2012) 032146.
[37] C. Galande, A.D. Mohite, A.V. Naumov, W. Gao, L. Ci, A. Ajayan, H. Gao, A. Srivastava, R.B. Weisman, P.M. Ajayan, Quasi-molecular fluorescence from graphene oxide, Sci. Rep. 1 (2011) 85.
[38] K.P. Loh, Q. Bao, G. Eda, M. Chhowalla, Graphene oxide as a chemically tunable platform for optical applications, Nat. Chem. 2 (2010) 1015–1024.
[39] G. Eda, M. Chhowalla, Chemically derived graphene oxide: towards large-area thin-film electronics and optoelectronics, Adv. Mater. 22 (2010) 2392–2415.
[40] J. Shang, L. Ma, J. Li, W. Ai, T. Yu, G.G. Gurzadyan, The origin of fluorescence from graphene oxide, Sci. Rep. 2 (2012) 792.
[41] C.T. Chien, S.-S. Li, W.J. Lai, Y.C. Yeh, H.A. Chen, I.S. Chen, L.-C. Chen, K.-H. Chen, T. Nemoto, S. Isoda, M. Chen, T. Fujita, G. Eda, H. Yamaguchi, M. Chhowalla, C.-W. Chen, Tunable photoluminescence from graphene oxide, Angew. Chem. Int. Ed. 51 (2012) 6662–6666.
[42] Z. Luo, P.M. Vora, E.J. Mele, A.T.C. Johnson, J.M. Kikkawa, Photoluminescence and band gap modulation in graphene oxide, Appl. Phys. Lett. 94 (11) (2009) 111909.